Marine Systems Supplement

Use of Jet-Flapped Hydrofoils as Ship Antipitching Fins

PAUL KAPLAN* AND THEODORE R. GOODMAN†
Oceanics Inc., Plainview, N. Y.

An analysis is presented to determine the feasibility of using jet flap hydrofoils as antipitching fins for large ships. The effectiveness of ordinary antipitching fins is limited by the occurrence of cavitation and/or ventilation, which leads to horizontal ship vibration associated with the cavity bubble collapse. It is shown that the jet flap postpones cavitation inception until the lift reaches two to three times the no-jet value. For an oscillating jet angle, it is shown that, at the encounter frequencies associated with wave orbital motions, the forces are quasi-steady and so is the condition for the inception of cavitation. Some considerations of the power requirements necessary to operate the jet flap are presented, and it is shown that the power expended to obtain a 25% decrease in pitch is a very small fraction of the total power available on an aircraft carrier of the Forrestal class.

Nomenclature

c	=	chord of foil
F	=	Froude number
g	=	acceleration caused by gravity
i	=	$(-1)^{1/2}$
$l(x)$	=	lift distribution on thin airfoil
n	=	reduced frequency [see Eq. (23)]
t	=	time
T	=	thrust
V	=	forward speed of foil
x	=	distance along foil measured from leading edge
α	=	geometric angle of incidence
γ	=	vorticity
δ	=	thickness ratio
ϵ	=	trailing edge slot opening
θ	=	ship pitch angle
$\dot{\theta}$	=	pitch rate
λ	=	wavelength
μ	=	$C_J/4$
ν	=	μn
ρ	=	fluid density
σ	=	cavitation number [see Eq. (1)]
τ	=	jet angle relative to foil chord
ω	=	wave frequency
φ	=	velocity potential
C_J	=	jet momentum coeff ($= M_J/\frac{1}{2}\rho V^2 c$)
C_L	=	lift coeff due to supercirculation
$\bar{C}_L$	=	total lift coefficient
C_{L_1}, C_{L_2}, C_{L_3}	=	see Eqs. (3) and (4)
$\bar{C}_M$	=	total moment coefficient
C_p	=	pressure coefficient
$C_{p\min}$	=	minimum pressure coefficient
C_T	=	thrust coefficient
$g(x')$	=	see Eq. (25)
h_0	=	displacement of jet
$h(x')$	=	see Eq. (25)
M_J	=	jet momentum
S_f	=	foil area
V_J	=	jet velocity
x'	=	see Eq. (26)
α'	=	see Eq. (6)
ω_e	=	frequency of encounter

Presented as Preprint 65-448 at the AIAA Second Annual Meeting, San Francisco, Calif., July 26–29, 1965; submitted August 20, 1965; revision received July 11, 1966. This work was carried out under the support of the Department of the Navy, Bureau of Ships, under Contract NObs-88418. [3.07, 7.07]

* President. Member AIAA.
† Vice-President. Associate Fellow AIAA.

Introduction

ONE of the obviously important (and limiting) motions of ships in waves is that of pitching. Much effort has been devoted toward developing designs of unorthodox ship forms to minimize these motions.[1] Other less drastic means have also been considered; the most prominent is that of fitting the ship with fins that act as dampers.[2] Motion reduction has been successful; nevertheless, certain problems are associated with these devices. In particular, there occurs a horizontal vibration of the hull caused by the cavity bubble collapsing on the fin.[3] This reduces the effectiveness of such devices.

What is required for application to pitch stabilization is a fin that provides large lift coefficients (hence large correcting pitch moment), and which is more resistant than standard hydrofoils to cavitation. One such device is a specially designed hydrofoil with a jet flap. The jet flap is a high-lift device originally applied to aircraft wings. It consists of a conventional wing with a thin jet blowing near the trailing edge at an angle relative to the foil chord. The downward component of jet momentum reacts to cause a lift. However, the jet also induces so-called "super-circulation" about the foil which produces an additional incremental lift. Thus, a high lift can be achieved simply by increasing the jet momentum or the jet angle or both. The pressure distribution caused by jet deflection is saddlebacked,[4] and there is a pressure peak near both leading and trailing edges. As a consequence, by comparison with the pressure distribution caused by angle of attack, which has a pressure peak only at the leading edge, the leading-edge pressure peak need not be so high for the same total lift. It follows that the adverse pressure gradient over the foil is smaller. Because of the reduced adverse pressure gradient, separation (and stall) are postponed to higher lift than that which can be achieved without the jet, and because of the reduced pressure peak, cavitation is also postponed to higher lift.

This paper presents an analysis of the inception of cavitation for a jet flap hydrofoil. It is shown on the basis of thin airfoil theory with thickness that the jet flap postpones cavitation until the lift reaches two to three times the no-jet value. Boundary-layer calculations were performed for every case considered, and in no case did separation occur; it is concluded that cavitation, and not separation, is the critical limiting condition for operation of the foil.

Because antipitching fins are required to operate in the oceanic environment, they are subject to the oscillatory

forces induced by waves. In any realistic pitch control system, the applied force must vary in response to the waves, and the simplest way to do this is to vary the jet angle. The frequencies associated with wave orbital velocities are shown to be sufficiently small so that the vorticity on the fin caused by an oscillatory jet angle is quasi-steady. The condition for unsteady operation on the threshold of cavitation is then also derived.

Finally, some consideration of the power requirements necessary to operate the jet flap are presented; and, for example, it is indicated that for an aircraft carrier of the Forrestal class, the power expended to obtain a 25% decrease in pitch motion can be expected to be a very small fraction of the total power available.

Cases Considered

In order to demonstrate the resistance to cavitation of a jet-flapped foil compared with an ordinary foil, certain numerical examples for specific conditions are worked out. For an antipitching fin mounted on a ship moving in waves, where the vertical wave orbital velocity acts both up and down during different parts of the wave cycle, the fin must produce lift in both directions. Consequently, the foil must be symmetrical. It is chosen to have an elliptical section for mathematical simplicity, and only two-dimensional foils are considered. These foils are then members of a one-parameter family, the parameter being the thickness ratio δ. Mixing of the jet with its surroundings will be neglected, since Kuchemann[4] has shown that there is only a small difference in the pressures with complete mixing as compared with the pressures with no mixing.

Associated with various operating conditions of forward speed, submergence, etc., is the cavitation index σ, which is defined by

$$\sigma = (P_\infty - P_v)/\tfrac{1}{2}\rho V^2 \tag{1}$$

where P_∞ is ambient pressure and P_v is vapor pressure. The nomograph presented in Ref. 5 can be used to determine the cavitation number. To avoid cavitation requires that the minimum pressure coefficient always exceed $-\sigma$. The study presented here considers foils on the threshold of cavitation, in which case the minimum pressure coefficient must equal $-\sigma$. For the numerical calculations herein, forward speeds of 21 and 29 knots (approximately 35 and 50 fps, respectively) were selected, leading to values of σ (for 5 ft submergence) of approximately 2.0 and 1.0.

Minimum Pressure

Spence[6] has formulated and solved the integral equation governing the flow about a jet-flapped foil using thin-airfoil theory. Kuchemann[4] used Spence's results to fit an assumed shape for the pressure distribution. Two different methods are proposed by Kuchemann. In the first, the over-all lift matches the given lift, and the distribution is symmetric about the midchord. In the second, both lift and thrust are matched, and the distribution is not symmetric. In both methods the exact distribution is approximated fairly far from the trailing edge. Kuchemann considers the second method to be superior to the first inasmuch as both lift and thrust are matched, and hence the second method was used in performing the computations herein. It was later discovered, however, that only the first method provides a true first approximation to Spence's theory. Nevertheless, the two methods yield results that differ by only 10% at most. In both methods the leading-edge singularity in the pressure distribution for an infinitely thin foil is of the correct form, as it is inversely proportional to the square root of distance from the leading edge. The trailing edge singularity assumed by Kuchemann is inversely proportional to the square root of distance from the trailing edge, which is not correct, because the true trailing edge singularity, as determined by Spence, is logarithmic. However, for our purposes, the Kuchemann curve fit for the pressure distribution will be adequate since the minimum pressure occurs near the leading edge for all cases studied. The pressure distribution on an elliptic foil of unit chord, based on Kuchemann's second method, is

$$C_P = 1 - \frac{(1+\delta)^2}{1 + [\delta^2(1-2x)^2/1 - (1-2x)^2]} \times \left[\cos\alpha' \pm \left\{\left[\frac{C_{L_1}}{2\pi} + \frac{C_{L_3}}{2\pi} + \sin\alpha'\right]\left(\frac{1-x}{x}\right)^{1/2} + \frac{C_{L_2}}{2\pi}\left(\frac{x}{1-x}\right)^{1/2}\right\}\right]^2 \tag{2}$$

where the upper (lower) sign refers to the upper (lower) surface.

The three lift coefficients C_{L_1}, C_{L_2}, C_{L_3} are determined from

$$C_{L_1} = C_{L_2} = \tfrac{1}{2}[(\partial C_L/\partial\tau)\tau - C_{L_3}] \tag{3}$$

$$C_{L_3} = \frac{2\pi C_J}{(\partial C_L/\partial\tau)\tau}(1 - \cos\tau) \tag{4}$$

where $(\partial C_L/\partial\tau)\tau$ = lift coefficient at zero angle of attack caused by supercirculation alone, i.e., neglecting the direct component due to jet momentum. The equation for $\partial C_L/\partial\tau$ is taken from Ref. 4,

$$\partial C_L/\partial\tau = 3.54\, C_J^{1/2} - 0.675 C_J + 0.156 C_J^{3/2} \tag{5}$$

The lift coefficient C_{L_3} is determined by matching the known thrust on the foil with the resultant of leading- and trailing-edge suctions. The thrust itself will be discussed more fully in a later section. Kuchemann's second method reduces to his first method when $C_{L_3} = 0$, in which case the thrust is not matched.

The quantity α' is determined from

$$\alpha' = (\alpha/2\pi)(\partial C_L/\partial\alpha) \tag{6}$$

where $\partial C_L/\partial\alpha$ = lift curve slope of jet flap foil. The equation for $\partial C_L/\partial\alpha$ is taken from Ref. 4 as follows:

$$\partial C_L/\partial\alpha = 2\pi + 1.152\, C_J^{1/2} + 1.106\, C_J + 0.51 C_J^{3/2} \tag{7}$$

Equations (2–7) completely specify the pressure distribution. It is seen, in general, that

$$C_p = C_p(x, \alpha, \tau, C_J, \delta) \tag{8}$$

If τ, C_J, and δ, are specified, then $C_p = C_p(x, \alpha)$, and the condition for minimum pressure is

$$(\partial C_p/\partial x)(x, \alpha) = 0 \tag{9}$$

Since the minimum pressure must equal the negative of the cavitation number,

$$-\sigma = C_p(x, \alpha) \tag{10}$$

Equations (9) and (10) comprise a set of two simultaneous equations for x and α. Applying Eq. (2), they lead to

$$\pm\left[1 + \frac{\delta^2(1-2x)^2}{4x(1-x)}\right][-(1-x)A_1 + xA_2] + \frac{\delta^2(1-2x)}{4x(1-x)}[\cos\alpha'(x)^{1/2}(1-x)^{1/2} \pm A_1(1-x) \pm A_2 x] = 0 \tag{11}$$

where

$$A_1 = (C_{L_1}/2\pi) + (C_{L_3}/2\pi) + \sin\alpha' \qquad A_2 = (C_{L_2}/2\pi)$$

An approximate solution for the location of the minimum pressure coefficient was developed, resulting in

$$x = (\delta^4/16)(\cos^2\alpha'/A_1^2) \tag{12}$$

which is valid for $A_1 > A_2$ and with the minimum pressure occurring near the leading edge. For negative angles of attack and for $C_{L_3} = 0$ (Kuchemann's first method), it is seen that $A_1 < A_2$; and in this case the first method predicts that the peak pressure lies near the trailing edge. There are local peaks in pressure near both leading and trailing edges for all α; for positive α the peak near the leading edge dominates, and for negative α this peak will actually continue to dominate for a certain range of α, but it is not possible, using the Kuchemann fit, to find the extent of this range. It will be assumed that the leading-edge peak dominates for both the analysis and the sample calculations.

By suppressing all lifting terms in Eq. (1), the limiting minimum pressure coefficient can be shown to be

$$C_{p\min} \leq -\delta(2 + \delta) \tag{13}$$

This result with the equality sign is presented in Ref. 5 for the nonlifting elliptic foil. In the neighborhood of this limit the approximation of Eq. (12) is invalid.

Pressure Distribution and Separation

As a check on the validity of Eq. (12), the pressure distribution [Eq. (1)] was programed on an IBM 1620 computer. The value of $C_{p\min}$ was observed to be within a few percent of $-\sigma$ for all cases, even though the value of x may have been in considerable error. Generally, the error in x was found to be greater for the thicker foils, but in that case the pressure distribution was flat so the error was of little significance in determining $C_{p\min}$. Typical pressure distributions are shown in Fig. (1).

It is clear that for the pressure distribution to be meaningful the boundary layer must be attached to the foil. Consequently, a boundary-layer calculation was performed for every case considered. The approximate method of Spence[7]

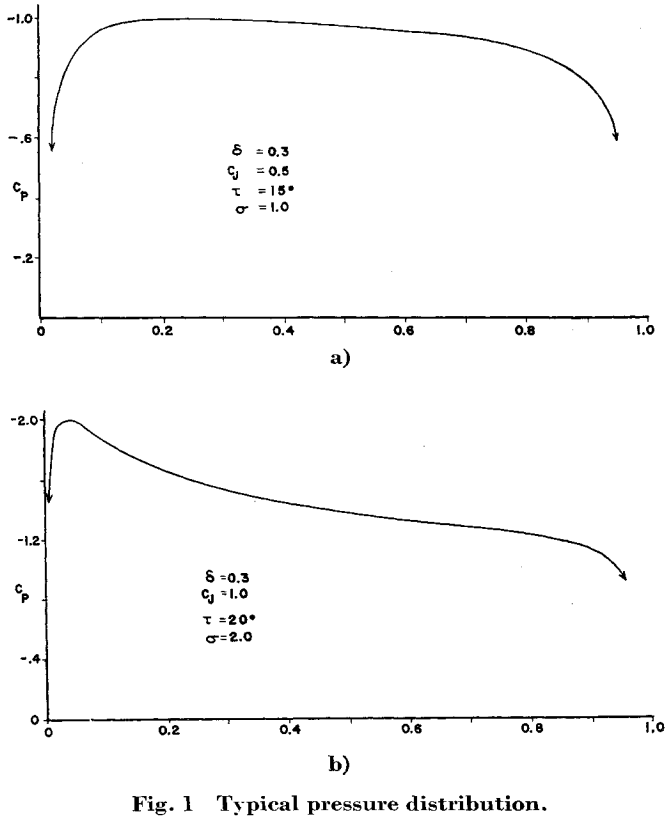

Fig. 1 Typical pressure distribution.

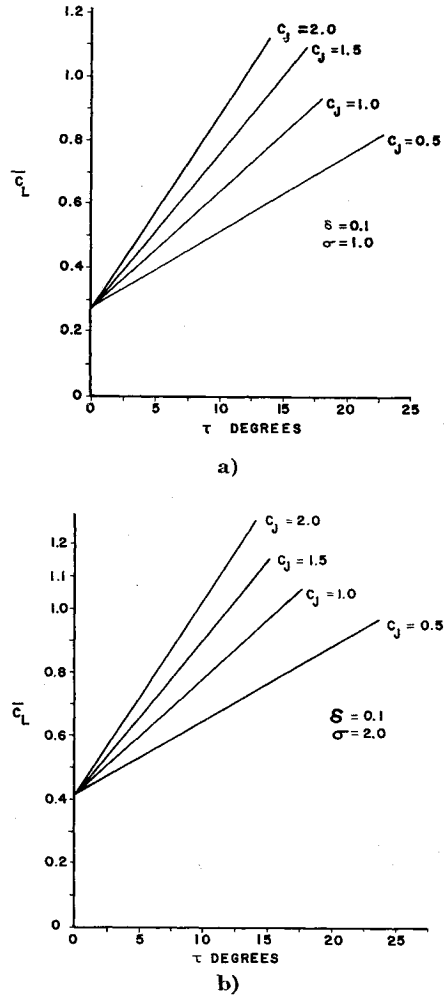

Fig. 2 Lift coefficient as a function of jet angle at the inception of cavitation.

was used to perform these calculations. They were performed on the IBM 1620 computer and were carried out for two Reynolds numbers, 2.2×10^7 and 3.0×10^7, which correspond to the two speeds 21 and 29 knots, respectively, for a foil chord of 12 ft. In each case the calculations were carried to within $0.05c$ of the trailing edge, and in no case did separation occur. Leading-edge separation is also deemed impossible because the foils have large nose radii.[6] It is concluded therefore that cavitation and not separation is the critical condition.

Total Lift, Thrust, and Moment

The total lift consists of three parts: the lift caused by vorticity induced by the jet, the lift caused by vorticity induced by the angle of attack, and the lift caused by jet momentum. The first two parts together are those caused by pressure on the external surfaces of the foil and are given by

$$(\partial C_L/\partial\alpha)\alpha + (\partial C_L/\partial\tau)\tau$$

for a thin foil. For a thick foil this expression must be modified by multiplying it by the factor $(1 + \delta)$. Thus, the total lift coefficient, including the contribution due to jet momentum, is

$$\bar{C}_L = [(\partial C_L/\partial\alpha)\alpha + (\partial C_L/\partial\tau)\tau](1 + \delta) + C_J\tau \tag{14}$$

where $\partial C_L/\partial\alpha$ is given by Eq. (7) and $\partial C_L/\partial\tau$ is given by Eq. (5).

For the foil thrust T, the thrust coefficient C_T is defined as

$$C_T = T/\tfrac{1}{2}\rho V^2 c \tag{15}$$

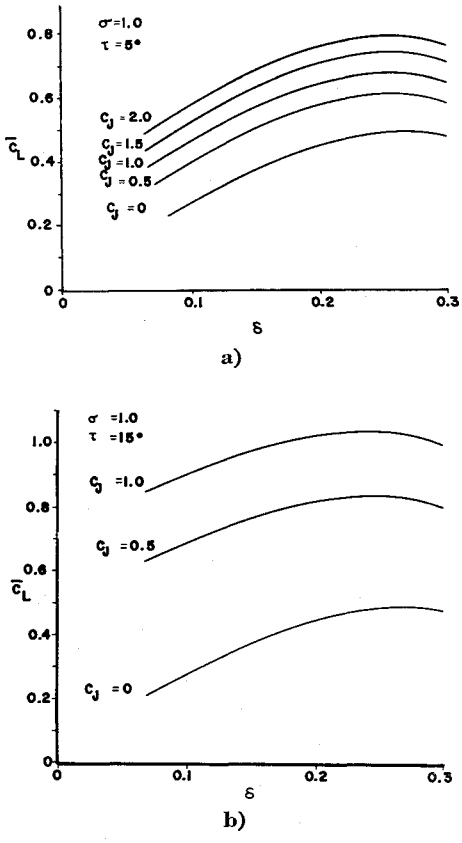

Fig. 3 Lift coefficient as a function of thickness ratio at the inception of cavitation.

Calling drag forces positive it can then be shown using the momentum theorem, that the thrust coefficient caused by pressures acting on the external surfaces of the foil is given by

$$C_T = -C_J(1 - \cos\tau) \tag{16}$$

On the other hand, the thrust coefficient caused by jet momentum is

$$C_T = -C_J \cos\tau$$

Hence the total thrust coefficient is

$$C_T = -C_J \tag{17}$$

which is independent of τ. Thus, complete jet momentum recovery is obtained in the form of thrust, according to theory.

An analysis of the foil leading-edge moment follows simply by integrating the lift distribution given by Kuchemann. The result for small angles α' and τ is

$$\bar{C}_M = \left\{\frac{1}{2}\frac{\partial C_L}{\partial \tau}\tau + \frac{\pi\alpha'}{2} + \frac{C_{L_3}}{4}\right\}(1 + \delta) + \tau C_J \tag{18}$$

The corresponding result using Kuchemann's first method can be obtained by setting $C_{L_3} = 0$ in Eq. (18), leading to

$$\bar{C}_M = \left\{\frac{1}{2}\frac{\partial C_L}{\partial \tau}\tau + \frac{1}{4}\frac{\partial C_L}{\partial \alpha}\alpha\right\}(1 + \delta) + C_J\tau \tag{19}$$

Equation (19) goes to the correct limit for small C_J as determined by Erickson,[8] whereas Eq. (18) has a 12.5% error imbedded within it. Erickson's result may be used as an alternative to that presented here provided it is properly modified for thickness effects.

Numerical Results

The lift coefficient and angle of attack at the inception of cavitation depend on the four parameters τ, C_J, σ, δ. Table 1 presents the values of these parameters that were used in the calculations. All permutations and combinations of these numerical values were used except if α became negative. In that case the first negative α which was achieved was retained, but higher values of C_J and/or τ, resulting in more negative α, were ignored.

Table 1 Numerical values of parameters used in calculations

τ	C_J	σ	δ
0°	0	1.0	0.1
5°	0.5	2.0	0.2
10°	1.0		0.3
15°	1.5		
20°	2.0		
25°			
30°			

Figures 2 and 3 present the results of the calculations for the lift. It is seen in Fig. 2 that the lift increases monotonically and almost linearly with jet angle in every case. The point at $\tau = 0$ from which the curves fan out is identically the lift obtained with no jet flap, i.e., just caused by foil angle of attack. It can be seen that increasing the jet angle creates lifts of double or triple the no-jet value without cavitating. From Fig. 3 it is seen that the lift is not monotonic with foil thickness but achieves a limiting maximum value. The thickness ratio at which this maximum occurs is an important feature for design use.

Plots of the angle of attack at the inception of cavitation are shown in Fig. 4. These curves correspond to the same conditions as those for the lift plotted in Fig. 2. As τ or C_J increases, the angle of attack is seen to decrease. This means that the more lift developed with the jet the less can

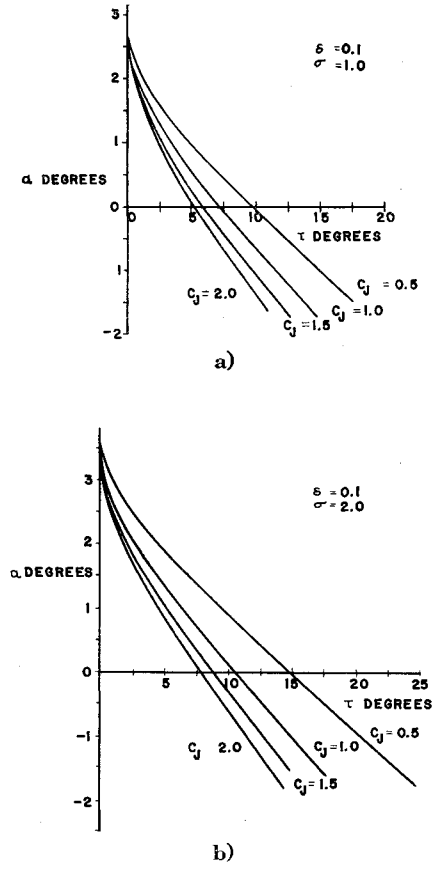

Fig. 4 Geometric angle of attack as a function of jet angle at the inception of cavitation.

be tolerated with angle of attack before cavitation sets in. In some cases at higher total lift it is necessary to generate negative lift due to angle of attack in order to compensate for the lift pressure peak generated by the jet. Despite the negative lift due to angle of attack, the total lift is always greater with the jet flap than without it.

Optimum Thickness Foils

It has been pointed out by referring to Fig. (3) that the lift achieves a maximum as a function of thickness ratio. By examining the numerical results it would appear that this optimum thickness is independent of both C_J and τ. Denoting it by δ_{opt}, it is seen to depend solely on cavitation number. It may thus be determined by setting $\tau = 0$, $C_J = 0$, which are, of course, the conditions that define a foil with no jet.

Figure 5 presents the lift, as a function of thickness ratio, at the inception of cavitation for certain cavitation numbers. These results are valid for the no-jet case, which, as has been indicated, is sufficient. The maximum lift with a jet will, of course, be higher than indicated on this figure. Each of the curves reaches a maximum at some value of thickness ratio, and a plot of δ_{opt} as a function of cavitation number, which is universal for elliptic foils, is presented in Fig. (6). Since the minimum pressure generally occurs near the nose of the foil, it is actually the nose radius that tends to lower the pressure peak and not the thickness. Of course, for an elliptic foil one parameter is a measure of the other, and for unit chord they are related according to

$$\text{nose radius} = \delta^2/2 \tag{20}$$

Discussion of Other Effects

The analysis and design procedure presented previously neglects a number of factors that may be of greater or lesser importance. Two of these have been mentioned already: jet mixing and finite aspect ratio. Two others are free surface effects and nonsteady effects. Nevertheless, the analysis as it stands has strongly demonstrated the utility of the jet flap foil as a device to produce high lift without cavitating. The effects of jet mixing and finite aspect ratio can be incorporated into the analysis using modifications of Eq. (1) suggested by Kuchemann.

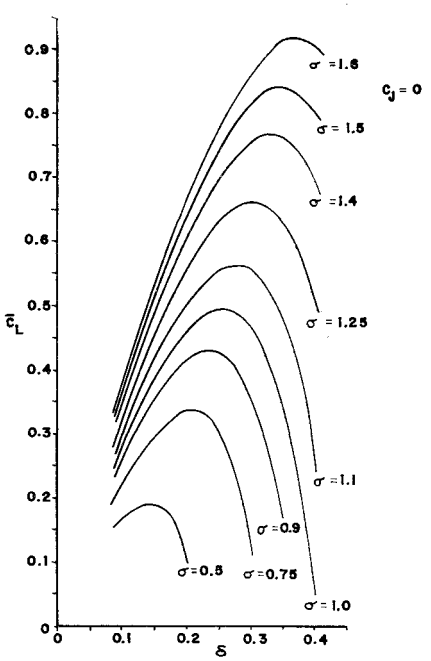

Fig. 5 Lift coefficient at the inception of cavitation, no jet.

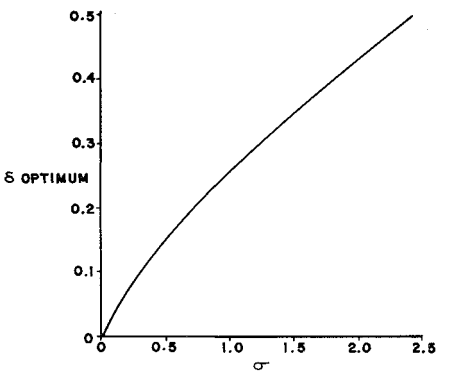

Fig. 6 Optimum foil thickness as a function of cavitation number.

The effect of the free surface may be important for jet-flapped hydrofoils, since they generally operate near the free surface and at speeds such that gravity effects are present. Because of gravity effects, simple wall or biplane results are not directly applicable. However, such studies may be informative.

A study of the effect of proximity to the ground for jet-flapped airfoils has been made by Williams, Butler, and Wood.[9] They report that when the jet impinges on the ground, a vortex forms below the airfoil and generates suction on the rear lower surface. This has a threefold effect, as follows: It limits further rise in C_L, leads to a rapid forward movement of the center of pressure (pitch-up), and causes substantial changes in thrust. Typically, at a ground clearance of one chord, this unfavorable ground effect becomes noticeable when C_J reaches about 1.5 for jet angles of the order of 60°. This C_J value is large and beyond the range of interest. Before impingement occurs, the effect on lift, pitching moment, and thrust are small. There is as yet no theoretical treatment of ground effect for jet-flapped wings.

It is possible that the jet itself will cavitate, or that it will aerate, sucking air down so that the flow becomes ventilated. This possibility is unlikely due to the nature of the pressure singularity. Near the leading edge, it is of square root type, but at the trailing edge it is logarithmic. Since the minimum pressure is always associated with the leading-edge singularity and since cavitation does not occur there, it is unlikely to occur where the singularity is weaker.

Some studies have been made of the flow about hydrofoils near a free surface at low submergences, e.g., the work of Parkin, Perry, and Wu.[10] These studies were carried out with conventional hydrofoils for which the lift was directed upward (toward the free surface). Those results show that hydrodynamic effects predominate over hydrostatic effects for the Froude numbers envisioned for jet-flapped foil systems, and that the incipient cavitation number is reduced when the hydrofoil runs closer to the free surface compared with the case with no free surface. Since the lift on the jet-flapped foil is directed downward, the upper surface pressure distribution can be expected to be less susceptible to cavitation compared with the results presented in Ref. 10. However, it is possible for the foil to "ingest" air through the surface, becoming ventilated, which is the major difficulty with previous antipitching fin installations (see Ref. 3). Although conditions for the occurrence of ventilation are not known as precisely as those for cavitation, it appears that an important adjunct to the occurrence of ventilation is for the flow to separate on the foil (see Ref. 11). Since a jet-flapped hydrofoil is highly resistant to separation, such a system appears to offer additional safety. No definite proof of ventilation resistance is given by these arguments, of course, and only an experimental study can determine whether ventilation will occur.

Finally, the effects of unsteadiness may be considered. A ship in waves is subject to oscillatory forces causing it to pitch, heave, etc., in an oscillatory manner. The analysis performed under steady-state assumptions is unrealistic for application to antipitching fins, although it was a necessary first step to establish the principle of cavitation postponement by the use of a jet flap. In the next section the limiting cavitation condition is derived for jet-flapped foils with an oscillating jet angle.

Forcing Frequency

The pitching motion that the fins must counteract occurs at a frequency ω_e called the frequency of encounter. This is greatest for a ship in head seas. In deep water,

$$\omega_e = \omega + (\omega^2 V/g) \tag{21}$$

and the wavelength of a gravity wave in deep water is given by

$$\lambda = 2\pi g/\omega^2 \tag{22}$$

The wavelengths likely to occur in the deep ocean lie between about 200 and 1200 ft. Hence, the wave frequencies will lie between 0.41 and 1.00 rad/sec. The ship forward speed V is again selected to be 35 and 50 fps, so that the range of ω_e is from 0.59 to 2.1 rad/sec for $V = 35$ fps, and from 0.67 to 2.6 for $V = 50$ fps. The reduced frequency, which is defined to be

$$n = \omega_e c/V \tag{23}$$

takes on the values (for a 12 ft chord) for $V = 35$ fps, $0.22 < n < 0.72$, whereas for $V = 50$ fps, $0.16 < n < 0.52$.

It may be concluded that for high-speed ships the reduced frequency over the entire range of wavelengths is of the order unity, i.e., $n = 0(1)$. Spence[12] has analyzed the flow and forces associated with an oscillating jet-flapped foil for the case $n = 0(1)$. His analysis therefore can be applied.

Integral Equation of Spence

In general, the angle of attack and the jet flap angle will both oscillate at the same reduced frequency n, although not necessarily in phase. For purposes of this study, however, the special case where the jet flap angle oscillates whereas the angle of attack remains steady will be considered. Because the problem is linear, two partial solutions will be superposed to obtain the complete solution. The first partial solution is for zero jet angle and constant angle of attack. This solution is steady, and can be obtained by setting $\tau = 0$ in the result presented earlier. The second partial solution is for zero angle of attack and oscillating jet angle. This second partial solution will be obtained from Spence.[12]

Spence's solution is restricted to small jet coefficient C_J, which is of practical importance for ship application. After making the transformation $\mu = C_J/4$, Spence shows that for small μ the coordinates can be stretched in such a way that the equations become independent of μ to the first order. Defining

$$\tau(t) = \tau_0 e^{inVt/c} \tag{24}$$

and with h_0 the displacement of the jet, and γ the vorticity in the jet, the solution for small μ is shown by Spence to be of the form

$$\begin{aligned} h_0(x, t) &= \mu c \tau_0 e^{inVt/c}(x/c)^{-1/2} h(x') \\ \gamma(x, t) &= 2U\tau_0 e^{inVt/c}(x/c)^{-1/2} g(x') \end{aligned} \tag{25}$$

where

$$x' = (x - c)/\mu c \tag{26}$$

Excluding terms of order μ and omitting the primes, Spence is led to seek a solution of the following system of integro-differential equations:

$$i\nu h + h' = -\frac{1}{\pi}\int_0^\infty \left(\frac{x}{\xi}\right)^{1/2} \frac{g(\xi)d\xi}{\xi - x} \tag{27}$$

$$i\nu g + g' = -h''' \tag{28}$$

where $\nu = \mu n$ and the boundary conditions are

$$h(0) = 0 \qquad h'(0) = 1 \tag{29}$$

If $n = 0(1)$, then $\nu \ll 1$ for small μ and the first approximation is obtained by setting $\nu = 0$, from which the basic steady equation

$$Lh'(x) = h'(x) - \frac{1}{\pi}\int_0^\infty \left(\frac{x}{\xi}\right)^{1/2} \frac{h''(\xi)d\xi}{\xi - x} = 0$$
$$h'(0) = 1 \tag{30}$$

is obtained. The solution to this equation is assumed known and will be denoted by $h_\infty(x)$. Following Spence, define

$$h(x) = h_\infty(x) + i\nu h_1(x) \tag{31}$$

and upon substituting into Eqs. (27–29), the solution for $h_1(x)$ was found by Spence to be

$$h_1'(x) = -2\int_0^x \xi h_\infty''(\xi)d\xi \tag{32}$$

This is as far as Spence carried the solution, but it is not sufficient for determining the pressure distribution on the foil. The next step is to determine the vorticity in the jet which is characterized by the function $g(x)$. Defining

$$g(x) = g_\infty(x) + i\nu g_1(x) \tag{33}$$

substituting into the previous equations, and equating like powers of ν, results in

$$g_\infty(x) = -h_\infty''(x) \tag{34}$$

and

$$g_1(x) = 2xh_\infty''(x) + h_\infty'(x) \tag{35}$$

In Eq. (16) of Ref. 12, Spence relates the vorticity on the wing to the vorticity in the jet,

$$\gamma(x, t) = \frac{1}{\pi}\left(\frac{c - x}{x}\right)^{1/2}\int_0^\infty \left(\frac{\xi}{\xi - c}\right)^{1/2} \frac{\gamma(\xi, t)}{\xi - x}\, d\xi$$
$$0 < x < c \tag{36}$$

which can be shown to lead to

$$\gamma(x, t) = \frac{\mu^{1/2}}{\pi}\left(\frac{c - x}{x}\right)^{1/2} 2V\tau_0 e^{inVt/c} \times \int_0^\infty \frac{g(\xi')d\xi'}{\xi'^{1/2}[1 + \mu\xi' - (x/c)]} \tag{37}$$

For small μ, the term $1 + \mu\xi' - (x/c)$ can be approximated by $1 - (x/c)$ and brought outside the integral provided $1 - (x/c) \neq 0(\mu)$, which means we must not be close to the trailing edge. Upon substituting the expression for $g(\xi')$,

$$\gamma(x, t) = \frac{2\mu^{1/2}}{\pi}\frac{V\tau_0 c}{[x(c - x)]^{1/2}} e^{inVt/c} \times \int_0^\infty \frac{[-h_\infty'' + i\nu(2\xi' h_\infty'' + h_\infty')]}{\xi'^{1/2}} d\xi' \tag{38}$$

where the first term is the quasi-steady vorticity and the term proportional to $i\nu$ represents the first-order unsteady correction. An integration by parts shows that the unsteady

correction is identically zero, and thus, to first order,

$$\gamma(x, t) = \gamma_\infty(x, t) \tag{39}$$

which is to say that for small jet momentum flux coefficient, and reduced frequencies of order unity, the vorticity on the wing is quasi-steady.

An explicit expression for the vorticity is found in the form

$$\gamma = \frac{2\mu^{1/2}}{\pi^{1/2}} \frac{V\tau_0 c}{[x(c-x)]^{1/2}} e^{inVt/c} \tag{40}$$

which may alternatively be written

$$\frac{2\gamma}{V} = \frac{2}{\pi} C_{L_1}\left(\frac{c-x}{x}\right)^{1/2} + \frac{2}{\pi} C_{L_2}\left(\frac{x}{c-x}\right)^{1/2} \tag{41}$$

where

$$C_{L_1} = C_{L_2} = \tfrac{1}{2}C_{L_0} \tag{42}$$

and

$$C_{L_0} = 4(\pi\mu)^{1/2}\tau_0 e^{inVt/c} \tag{43}$$

Here, C_{L_0} is the total pressure-induced lift, i.e., the part caused by supercirculation alone.

Methods of Kuchemann

The foregoing equations are precisely the first method of Kuchemann[4] (without thickness correction) for the approximate lift distribution on a jet-flapped foil. Kuchemann considered his second method to be more refined than his first and therefore favored it. It will be shown, however, by comparing three aspects of Kuchemann's two methods, that the first method is superior.

The first comparison was given in a previous section where the limiting moment coefficient for small C_J was determined and compared to results of Erickson,[8] showing exact agreement only for the first method.

The second comparison concerns the suctions at leading- and trailing edges from which Kuchemann determines C_{L_3}. The trailing edge singularity is assumed by Kuchemann to be of the form $(c-x)^{-1/2}$, whereas it is actually of the form $\log(c-x)$ according to exact linear theory. Hence, there is, in fact, no suction at the trailing edge at all, and the thrust must be obtained solely from the leading-edge suction. From this, it necessarily follows that $C_{L_3} = 0$.

The third comparison will be made after developing an expression for the nonsteady lift distribution. According to linearized theory the pressure jump in unsteady flow is

$$\Delta C_p = (2/V)[\gamma + (1/U)(\partial\Delta\varphi/\partial t)] \tag{44}$$

where $\Delta\varphi$ is the jump in potential and is given by

$$\Delta\varphi = \int_0^x \gamma(\xi, t)d\xi \tag{45}$$

Substituting Eq. (40) into Eqs. (44) and (45) yields

$$\Delta C_p = 4(\mu)^{1/2}\tau_0 e^{inVt/c}\frac{c}{[x(c-x)]^{1/2}} + 2\,in\,\sin^{-1}\left(\frac{x}{c}\right)^{1/2} \tag{46}$$

leading (by integrating over the chord of the foil) to the lift coefficient

$$C_{L_0} = 4(\mu\pi)^{1/2}\tau_0 e^{inVt/c}\left[1 + \frac{in}{2}\right] \tag{47}$$

which is precisely Spence's result for small μ. Thus, the vorticity distribution, [Eq. (40)] leads to the correct in-phase and out-of-phase lift to first order. When a nonzero C_{L_3} is introduced, the in-phase component of the lift is still correct because it has been compelled to be, but the out-of-phase component is not.

By analogy with the steady distribution, the pressure jump may be written

$$\Delta C_p = \frac{2}{\pi} C_{L_1}\left(\frac{c-x}{x}\right)^{1/2} + \frac{2}{\pi} C_{L_2}\left(\frac{x}{c-x}\right)^{1/2} + \frac{2}{\pi}(C_{L_1} + C_{L_2})\,in\,\sin^{-1}\left(\frac{x}{c}\right)^{1/2} \tag{48}$$

where C_{L_1}, C_{L_2} are defined by Eq. (42).

Distribution of Pressure on a Thick Foil

Equation (48) has been derived on the basis of thin airfoil theory. But just as in the steady case, a correction may be applied to account for thickness. Kuchemann used the method of Weber[13] to obtain this correction, but since this method was derived for steady flow, a different procedure is required for the unsteady case. Weber's method consists in reconstructing the nonlinear pressure term in Bernoulli's equation and then correcting it so as to eliminate the singularity which appears at the leading edge in the linearized version, but which is actually not present. For the unsteady case this may be interpreted to mean that the in-phase component should be reconstructed but the out-of-phase component remains unaltered since it is not singular. Before reconstructing the pressures, the partial solution for zero jet angle and constant angle of attack must be added. Thus, the complete linearized pressure jump is

$$\Delta C_p = 4\left[\left(\frac{C_{L_1}}{2\pi} + \alpha'\right)\left(\frac{c-x}{x}\right)^{1/2} + \frac{C_{L_2}}{2\pi}\left(\frac{x}{c-x}\right)^{1/2} + \left(\frac{C_{L_1} + C_{L_2}}{2\pi}\right) in\,\sin^{-1}\left(\frac{x}{c}\right)^{1/2}\right] \tag{49}$$

and upon reconstructing the nonlinear pressures, the result is

$$C_p = 1 - \frac{(1+\delta)^2}{1 + [\delta^2(1-2x)^2/1 - (1-2x)^2]} \times \left[1 \pm \left\{\frac{C_{L_1}}{2\pi}\cos\frac{nVt}{c} + \alpha'\right\}\left(\frac{1-x}{x}\right)^{1/2} + \frac{C_{L_2}}{2\pi}\cos\frac{nVt}{c}\left(\frac{x}{1-x}\right)^{1/2}\right]^2 \pm 2n\left(\frac{C_{L_1}}{2\pi} + \frac{C_{L_2}}{2\pi}\right) \times \sin^{-1}(x)^{1/2}\sin\frac{nVt}{c} \tag{50}$$

where the chord is unity, the solution is now real, and $\tau = \tau_0\cos(nVt/c)$. Furthermore, C_{L_1} and C_{L_2} are redefined as follows:

$$C_{L_1} = C_{L_2} = \tfrac{1}{2}C_{L_0} = \tfrac{1}{2}\tau_0[2(\pi C_J)^{1/2} - 0.675C_J + 0.156C_J^{3/2}] \tag{51}$$

Minimum Pressure in the Unsteady Case

The minimum pressure controls cavitation, and the two conditions which control the position along the chord and the time during the cycle of the minimum are

$$\partial C_p/\partial x = 0 \qquad \partial C_p/\partial t = 0 \tag{52}$$

In the steady case, the minimum pressure has been shown to occur near the leading edge, and for reduced frequencies of order unity it may be expected that the minimum pressure will also be near the leading edge. For small x, however, the out-of-phase component of the pressure is small, as can be seen from Eq. (50); and a simple analysis demonstrates that the minimum pressure is indeed directly in phase with the jet angle. The location of the minimum pressure is then

determined from

$$\partial C_p/\partial x = 0 \tag{53}$$

where C_p is determined from Eq. (50) by setting $nVt/c = 0$. The resulting equation is precisely the steady-state pressure coefficient with the jet angle τ replaced by the amplitude of the jet angle oscillation; i.e., it is identically Eq. (2). The problem thus has been reduced to the steady problem, and all of the numerical work previously presented applies.

The total lift for a thin foil with an oscillating jet is given by Eq. (47). Since only the in-phase component of the pressures has been corrected for thickness, it follows that the in-phase component of the total lift should be corrected for thickness. According to Weber, and as applied by Kuchemann, this correction is obtained by multiplying the thin foil result by the factor $(1 + \delta)$. Thus, the in-phase component must be multiplied by this factor. However, Woods[14] has shown that the effect of thickness on unsteady airfoil results can be obtained by replacing the reduced frequency n by $n(1 + \delta)$. Thus, the effect of thickness can be fully accounted for by multiplying both the in-phase and out-of-phase components by the factor $(1 + \delta)$, leading to

$$\bar{C}_L = \left[\frac{\partial C_{L_0}}{\partial \tau}\left(1 + \frac{in}{2}\right)\tau(t) + \frac{\partial C_L}{\partial \alpha}\alpha\right](1 + \delta) + C_J\tau(t) \tag{54}$$

where $\partial C_{L_0}/\partial\tau$ is the quasi-steady value for a thin foil due to supercirculation alone.

In a similar manner, by evaluating the integral

$$\bar{C}_M = \int_0^1 xC_p dx + C_J\tau(t) \tag{55}$$

the unsteady leading-edge moment coefficient is found to be

$$\bar{C}_M = \left[\frac{\partial C_{M_0}}{\partial \tau}\left(1 + \frac{5}{16}in\right)\tau(t) + \frac{\partial C_M}{\partial \alpha}\alpha\right](1 + \delta) + C_J\tau(t) \tag{56}$$

where $\partial C_{M_0}/\partial\tau$ is the quasi-steady value for a thin foil due to supercirculation alone.

Power Requirements for Pitch Stabilization Application

One of the major considerations to determine the feasibility of applying jet-flapped hydrofoils is the power requirement. This quantity determines the necessary equipment, space, etc., needed for such a system, and also determines the portion of available propulsive horsepower that must be siphoned off to attain stabilization. Because of this power penalty, it appears to be most practical to consider applications wherein pitch reduction is a vital aspect of the operational capabilities of the ship, and where there is a large amount of power available. The application that fits these requirements is the large attack aircraft carrier, where pitch reduction of approximately 0.50° will make a significant improvement in aircraft landing capability (see data in Ref. 15).

The jet-flap hydrofoil system used as an antipitching fin is envisioned to be made up of two separate foils mounted on the ship hull near the bow. The angular orientation of the jet is controllable using a cam. Water is taken in through openings at the bow, transported via appropriate ducting by auxilliary pumps, and ejected through the trailing edge jets. Ram pressure is used to build up the head within the pump so as to resist pump cavitation. The jet angle can be controlled or programed so as to develop maximum stabilizing action in accordance with the ship motions in a particular seaway.

An application is chosen with a total stabilizer area of 1000 ft², which is about 1% of the waterplane area of a Forrestal class carrier. The jet efflux opening is selected to be $\epsilon = 0.02c$, and the jet velocity is such that the jet momentum coefficients $C_J = 0.09$ (for 50 fps forward speed) and 0.16 (for a forward speed of 35 fps). The flow rate $Q = 1400 - 1500$ ft³/sec, and the pump power required to overcome the head loss is approximately 9000 hp. For the lower (higher) speed the lift coefficient developed by the foil is $\bar{C}_L = 1.0$ (0.50), and this can be achieved with a foil having a thickness ratio $\delta = 0.20 - 0.30$ without cavitation.

The power expended to create the required jet momentum is not completely lost, since jet thrust recovery is achieved [see Eq. (17)]. The thrust hypothesis for jet flaps has been verified in a number of experimental studies.[16,17] However, this result is valid only for the limiting case of extremely large jet velocities relative to the freestream, and ignores the manner in which fluid carried in the jet is introduced. For the jet-flapped system, water will be taken in at the bow of the ship, and then pumped to higher speed to form the jet. The thrust recovered under these circumstances is the same as in a standard jet propulsion system, and is independent of the deflection angle. The thrust power recovered is found to be approximately 6500 hp. Thus a net expenditure of about 2500 hp is necessary for obtaining this particular performance, neglecting losses due to friction, mixing, pump efficiency, etc.

With regard to the selection of the pumps, the choice was based on the performance of a series of homologous pumps[18] using the characteristics of existing efficient pumps as a base. An axial flow pump was first considered, but the final choice was a mixed flow pump whose characteristics are determined by the same method of design. This pump has a small tip speed that tends to avoid pump cavitation. Other losses were evaluated, namely, entrance loss, head loss in bends, friction loss in the conduit and the foil ducting, etc. These increased the total power expenditure to about 13,000 hp. Allowing for thrust recovery power, the net power expenditure is then about 6000 hp, which is in the range of 2–3% of the total shaft horsepower of a large aircraft carrier. Other considerations such as additional equipment space requirements noise effects etc. must also be weighed before the over-all effectiveness of such a system can be ascertained.

The power expenditures determined previously were used to achieve a certain lift without cavitation. The question now arises as to the resultant stabilizing capability achieved. Assuming $\bar{C}_L = 1.0$ and $x_f = 500$ ft, the jet-flapped foil will create a stabilizing moment, at a forward speed of 35 fps, given by

$$M_f = \frac{\rho}{2} 2S_f V^2 \bar{C}_L x_f = \rho S_f V^2 x_f \bar{C}_L = 0.61 \times 10^9 \text{ lb-ft} \tag{57}$$

where x_f is the moment arm measured from the carrier c.g.

The magnitude of the stabilizing moment given in Eq. (57) is approximately 25% of the wave-induced pitching moment on the USS Forrestal for 10 ft high waves having a wavelength in the range $0.75 < \lambda/L < 1.0$. Such a wave excites the maximum pitch motion of the Forrestal at a 20-knot forward speed in head seas (near resonance, see Ref. 19). In addition to this 25% pitch motion reduction there is also a contribution to pitch damping caused by the fixed antipitch fin effect, resulting in a damping moment given by

$$M_d = \rho S_f V \frac{2\pi}{1 + (2/AR)} x_f{}^2\dot{\theta} \tag{58}$$

whose numerical value is $32.8 \times 10^9\dot{\theta}$. This particular magnitude increases pitch damping by about 15%. Thus, the fixed fin effect and the direct jet-developed control pitch moments both act to reduce pitching motion. At higher forward speeds greater reduction is achieved.

Conclusions

As a result of this study, certain conclusions are evident, and they are listed below, as follows.

1) Cavitation, not separation, is the critical limiting flow condition.

2) Lift coefficients of two to three times the no-jet value can be achieved with a jet flap without cavitating.

3) Maximum lift can be achieved without cavitation using a foil of optimum thickness; this optimum thickness is solely a function of the cavitation index.

4) The lift developed for the case of constant angle of attack and oscillating jet angle will be cavitation-limited at the quasi-steady values of jet angle determined by steady flow considerations, for the range of low reduced frequencies arising from a ship encounter with wave orbital velocities.

5) Jet-flap hydrofoils can provide useful pitch stabilization without the dangers associated with cavitation. The power penalty is a small percentage of the total propulsive power of a large ship such as an aircraft carrier. Also, additional equipment that occupies space and adds complexity must be installed.

References

[1] Boericke, H., Jr., "Unusual displacement hull forms for higher speeds," Intern. Shipbuilding Prog. **6** (1959).

[2] Abkowitz, M. A., "The effect of antipitching fins on ship motions," Trans. Soc. Naval Architects Marine Engrs. **67,** 210–252 (1959).

[3] Ochi, K. M., "Hydroelastic study of a ship equipped with an antipitch fin," Trans. Soc. Naval Architects Marine Engrs. **69,** 281–337 (1961).

[4] Kuchemann, D., "A method for calculating the pressure distribution of jet flapped wings," Great Britain Aeronautical Research Council R & M 3036 (1956).

[5] Breslin, J. P. and Landweber, L., "A manual for calculation of inception of cavitation on two and three dimensional forms," Soc. Naval Architects Marine Engrs. T&R Bull. 1-21 (1961).

[6] Spence, D. A., "The lift coefficient of a thin, jet-flapped wing," Proc. Roy. Soc. **A238,** 46–68 (1956).

[7] Cooke, J. C. and Brebner, G. G., "The nature of separation and its prevention by geometric design in a wholly subsonic flow," *Boundary Layer and Flow Control* (Pergamon Press, New York, 1961), Vol. I, pp. 144–185.

[8] Erickson, J. C., Jr., "The pitching-moment coefficient of a jet-flapped thin airfoil," J. Aerospace Sci. **29,** 1489–1490 (1962).

[9] Williams, J., Butler, S. F., and Wood, M. N., "The aerodynamics of jet flaps," Great Britain Aeronautical Research Council R & M 3304 (1963).

[10] Parkin, B. R., Perry, B., and Wu, T. Y., "Pressure distribution on a hydrofoil near the water surface," J. Appl. Phys. **27,** 232–240 (1956).

[11] Wadlin, K. L., "Mechanics of ventilation inception," *Proceedings of the 2nd Symposium on Naval Hydrodynamics* (Office of Naval Research, Washington, D. C., 1958).

[12] Spence, D. A., "Theory of the jet-flap for unsteady motion," J. Fluid Mech. **10,** Pt. 2, 237–258 (1961).

[13] Weber, J., "Calculation of the pressure distribution over the surface of two-dimensional and swept wings with symmetrical aerofoil sections," Great Britain Aeronautical Research Council R&M 2918 (July 1953).

[14] Woods, L. C. "The lift and moment acting on a thick aerofoil in unsteady motion," Phil. Trans. Roy. Soc. (London) **A295,** 131–162 (1954).

[15] Durand, T. S. and Teper, G. L., "An analysis of terminal flight path control in carrier landing," Systems Technology Inc., Rept. 137-1 (August 1964).

[16] Foley, W. M., "An experimental study of jet-flap thrust recovery," Stanford Univ., Dept. Aeronautical Engineering Rept. 136 (July 1962).

[17] Korbacher, G. K., "Performance and operation of quasi two-dimensional jet flaps," Institute of Aerophysics, Univ. of Toronto, Rept. 90 (May 1963).

[18] Russell, G. E., *Hydraulics* (Henry Holt and Company, New York, 1948), 5th ed., 430–438.

[19] Kaplan, P. and Sargent, T. P., "Theoretical study of the motions of an aircraft carrier at sea," Oceanics Inc. Rept. 65-22 (January 1965).